Evidence from ^{18}O Exchange Measurements for Steps Involving a Weak Acid and a Slow Chemical Transformation in the Mechanism of Phosphorylation of the Gastric H^+,K^+-ATPase by Inorganic Phosphate†

Larry D. Faller* and Ruben A. Diaz

The Center for Ulcer Research and Education, Department of Medicine, UCLA School of Medicine and Veterans Administration Hospital Center, Los Angeles, California 90073

Received December 5, 1988; Revised Manuscript Received April 17, 1989

ABSTRACT: Phosphorylation of the gastric H,K-ATPase by P_i has been studied by measuring the $P^{18}O_j{}^{16}O_{4-j}$ distribution as a function of time at different H^+, K^+, and $[^{18}O]P_i$ concentrations. The advantage of isotope exchange measurements is that the $P^{18}O_j{}^{16}O_{4-j}$ distribution depends on the relative rates of HOH loss to form the phosphoenzyme intermediate and P_i dissociation from the enzyme. Therefore, ^{18}O exchange is a sensitive probe of mechanism. K^+ increases the exchange rate (v_{ex}) but does not affect the partition coefficient (P_c) that determines the $P^{18}O_j{}^{16}O_{4-j}$ distribution. Conversely, H^+ inhibits exchange. A single P_c describes the data at every pH, but the value increases from 0.04 at pH 8 to 0.64 at pH 5.5. v_{ex} depends hyperbolically on $[P_i]_0$. K_m for P_i does not depend on pH, and P_c does not depend on $[P_i]_0$. Individual rate constants in the phosphorylation mechanism are estimated. Formation of the $E{\cdot}P_i$ complex that looses HOH is 1-2 orders of magnitude slower at pH 5.5 than at pH 8 and is not diffusion controlled. The observed change in P_c with pH is compatible with catalysis occurring by a different mechanism when a group with $pK_a = 7.2$ is protonated. Slower than diffusion-controlled formation of the $E{\cdot}P_i$ complex that splits out HOH is evidence for a relatively slow, unimolecular chemical transformation involving an additional intermediate in the phosphorylation mechanism, such as a protein conformational change.

The Mg^{2+}-dependent, H^+-transporting, and K^+-stimulated adenosine-5′-triphosphatase (H,K-ATPase)[1] isolated from gastric epithelia also catalyzes ^{18}O exchange between P_i and HOH (Faller & Elgavish, 1984). The ionic requirements for isotope exchange, inhibition of the reaction, and the exchange rate are all compatible with catalysis of medium[2] ^{18}O exchange via the same phosphoenzyme intermediate implicated in catalysis of ATP hydrolysis. Therefore, isotope exchange is an alternative way of studying the terminal steps in the overall catalytic mechanism. The advantage of ^{18}O exchange is that information about the reaction pathway, as well as the phosphorylation rate, can be obtained from measurements of the $P^{18}O_j{}^{16}O_{4-j}$ distribution as a function of time.

The effects of P_i concentration and of the transported ions, H^+ and K^+, on catalysis of medium ^{18}O exchange by the gastric H,K-ATPase have been studied. Two principal experimental observations are reported. First, the $P^{18}O_j{}^{16}O_{4-j}$ distribution changes dramatically with pH. This result was communicated earlier in an abstract (Faller, 1987). Second, the rate of formation of the enzyme–inorganic phosphate complex that looses water to form the covalent phosphoenzyme intermediate decreases with pH, becoming slower than diffusion controlled. These results are interpreted as evidence for steps involving a weak acid and a relatively slow chemical transformation in the phosphorylation mechanism.

Experimental Procedures

Materials

H,K-ATPase. Microsomal vesicles rich in H,K-ATPase were isolated from hog stomachs and purified by zonal centrifugation as previously described (Faller, 1989b). The specific activity of enzyme in broken vesicles from the lighter fraction averaged 148 ± 23 μmol mg^{-1} h^{-1} ($n = 4$). The phosphorylation capacity of the preparation is 1.5 ± 0.3 nmol mg^{-1} (Faller et al., 1983). The stoichiometry of nucleotide and inhibitor binding is approximately twice the maximum phosphorylation level (Faller, 1989a) but still less than half the theoretical stoichiometry for a 114-kDa protein (Shull & Lingrel, 1986). Nevertheless, strict linearity between specific ATPase activity and the ^{18}O exchange rate indicates that neither unassociated low molecular weight polypeptides in the preparation nor inactive 114-kDa proteins affect the reactivity of functional H,K-ATPase molecules (Faller & Elgavish, 1984). A single partition coefficient for ^{18}O exchange was measured at every pH in this study, providing additional evidence for homogeneity of the enzyme that turns over.

Labeled P_i. $[^{18}O]P_i$ was prepared as described by Boyer and co-workers (Hackney et al., 1980; Stempel & Boyer, 1986). Briefly, phosphorus pentachloride was reacted in a dry box with a 20-fold excess of >98.5% enriched $H^{18}OH$. After neutralization with imidazole and recovery of the unreacted $H^{18}OH$ by vacuum transfer, phosphoric acid was isolated from the reaction mixture by chromatography on an AG1-X4 ion

† This work was supported by National Science Foundation Grants DMB 83-09756 and 87-04525 and U.S. Public Health Service Grant DK 36873.

[1] Abbreviations: H,K-ATPase, Mg^{2+}-dependent, H^+-transporting, and K^+-stimulated ATPase (EC 3.6.1.3); Na,K-ATPase, Mg^{2+}-dependent and Na^+- and K^+-stimulated ATPase; Ca-ATPase, Ca^{2+}- and Mg^{2+}-dependent ATPase; SR, sarcoplasmic reticulum; MES, 2-(*N*-morpholino)ethanesulfonic acid; DMSO, dimethyl sulfoxide; TNP-ATP, 2′,3′-*O*-[(2,4,6-trinitrophenyl)cyclohexadienylidine]-ATP; FITC, fluorescein 5′-isothiocyanate; proflavin, 3,6-diaminoacridine; vanadate, $H_2VO_4^-$; P_i, inorganic phosphate; $[^{18}O]P_i$, ^{18}O-enriched P_i; $P^{18}O_j{}^{16}O_{4-j}$ ($0 \leq j \leq 4$), ^{18}O isotopomers of P_i; AE, average isotope enrichment; SA, specific activity; MW, molecular mass; GCMS, gas chromatography–mass spectrometry; NMR, nuclear magnetic resonance.

[2] "Medium" exchange is used to contrast isotope exchange between medium P_i and HOH with "intermediate" exchange, in which the P_i is generated in situ as an intermediate in the hydrolysis of ATP.

0006-2960/89/0428-6908$01.50/0

exchange column. The product is stored as the lyophilized sodium salt. GCMS analysis indicated 89.0% $P^{18}O_4$, 10.5% $P^{18}O_3{}^{16}O_1$, and 0.5% $P^{18}O_2{}^{16}O_2$ and NMR analysis gave 89.1% $P^{18}O_4$ and 10.9% $P^{18}O_3{}^{16}O_1$, which correspond to average isotope enrichments[3] of 97.1% and 97.3%, respectively.

Reagents. Ultrapure, dry PCl_5 was obtained from Alfa Products and >98.5% ^{18}O-enriched $H^{18}OH$ from Stohler/KOR. Vanadate-free ATP and pNPP were purchased from Sigma. D_2O from Aldrich Chemical Co. was used. All other reagents were of the highest grade available.

Methods

Protein. The protein (P_0) in gastric vesicle suspensions was quantified ($\mu g\ mL^{-1}$) by the biuret reaction with bovine serum albumin as a standard (Lowry et al., 1951).

Inorganic Phosphate. The amount of P_i in $[^{18}O]P_i$ stock solutions, or formed as a function of time during catalysis of ATP hydrolysis, was quantified by forming the phosphomolybdate complex, extracting into butyl acetate, and comparing the absorbance at 320 nm to the absorbance of extracts from standard KH_2PO_4 solutions (Yoda & Hokin, 1970). The distribution of ^{18}O in inorganic phosphate was measured by NMR or GCMS.

NMR. NMR spectra were obtained with a 11.75-T Bruker instrument at a frequency of 202.5 MHz for ^{31}P by averaging 48 free induction decays over 197 s and calculating the Fourier transform. Substituting a ^{18}O atom for a ^{16}O atom in P_i causes a 4.5-Hz chemical shift. The individual peaks were base line resolved, so the percentage contribution of each of the five $P^{18}O_j{}^{16}O_{4-j}$ species to the spectrum could be evaluated directly from the peak heights.

The advantage of the ^{31}P NMR method for analyzing the distribution of ^{18}O in P_i (Cohn & Hu, 1978) is that isotope exchange can be followed in real time. $[^{18}O]P_i$ adjusted to pH 7.4 was passed through a Chelex 100 column to remove paramagnetic ions, and the concentration of P_i in the stock solution was measured; 2.5 mL of reaction mixture (see figure legends for compositions) containing 10–20 mM $[^{18}O]P_i$ in a 10 mm diameter quartz NMR tube was adjusted to the desired pH. After the initial distribution of ^{18}O in P_i was measured, exchange was initiated by adding a small aliquot of enzyme, and the reaction was followed by remeasuring the isotope distribution at approximately 15-min intervals. The disadvantage of NMR is that millimolar concentrations of P_i are required for analysis because of the low sensitivity of the phosphorus nucleus.

GCMS. The disadvantage of GCMS is that the reaction must be quenched and the P_i isolated for analysis, so it is impractical to determine as many time points as in an NMR experiment. The advantage of measuring the isotope distribution by mass spectrometry is that as little as 50 nmol of $[^{18}O]P_i$ can be analyzed. Exchange was initiated by adding enzyme to a large enough volume of assay solution to contain ≥150 nmol of $[^{18}O]P_i$. The reaction was quenched with an equal volume of methanol, and the $[^{18}O]P_i$ was isolated by ion exchange chromatography.

The procedure developed by Stempel and Boyer (1986) was used to measure the $P^{18}O_j{}^{16}O_{4-j}$ distribution. Briefly, the volatile triethyl phosphate formed by reaction with diazoethane was chromatographed on a J & W Scientific Inc. DB-WAX megabore column and analyzed with a Hewlett-Packard 5995 mass spectrometer operated in the specific-ion monitoring mode. The instrument was tuned for optimal detection of the fully protonated diethyl phosphate fragments ranging in mass from 155 to 163. Correction for spillover from completely unprotonated diethyl phosphate was based on the contribution of mass 153 (about 5%) to the spectrum of a natural isotope abundance standard.

[3] AE = $\sum_j P^{18}O_j{}^{16}O_{4-j}/4\sum_j P^{18}O_j{}^{16}O_{4-j}$ $(0 \le j \le 4)$.

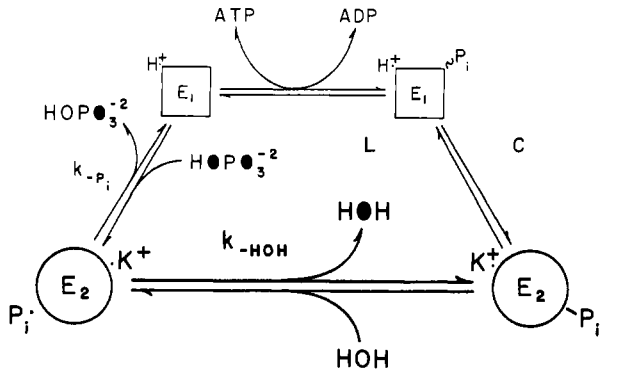

FIGURE 1: Conformational model of catalysis and transport. Two enzyme conformations can explain coupled, vectorial transport (Jencks, 1980). This is shown diagrammatically for the H,K-ATPase. The "high-energy" conformer (E_1) reacts with ATP and ADP. Its transport site is exposed to the cytosol (C) and binds H^+ tighter than K^+. Conversely, the "low-energy" conformer (E_2) reacts with P_i and HOH. Its transport site is exposed to the lumen (L) and binds K^+ tighter than H^+. ^{18}O (●) exchange is catalyzed by E_2.

Data Analysis. Assuming free rotation of noncovalently bound P_i ($E{\cdot}P_i$), the probability of the covalent phosphoenzyme intermediate (E–P) re-forming before P_i dissociates from the enzyme depends on the relative rates of water and P_i loss (k_{-HOH} and k_{-P_i} steps in Figure 1). In the simplest case of a single reaction intermediate

$$E + P_i \underset{k_{-1}}{\overset{k_1}{\rightleftharpoons}} E{\cdot}P_i \underset{k_{-2}}{\overset{k_2}{\rightleftharpoons}} E\text{–}P + HOH \quad (1)$$

the partition coefficient (P_c) is

$$P_c = k_2/(k_{-1} + k_2) \quad (0 \le P_c \le 1) \quad (2)$$

P_c is related to the pseudo-first-order rate constants (k') for the disappearance of $P^{18}O_4$ and AE by (Hackney & Boyer, 1978)

$$P_c = (1/3)[4 - k'(P^{18}O_4)/k'(AE)] \quad (3)$$

$k'(P^{18}O_4)$ and $k'(AE)$ were determined from semilogarithmic plots of percent $P^{18}O_4$ and percent AE versus time. Hackney (1980) has derived equations for calculating the percentage of each of the five $P^{18}O_j{}^{16}O_{4-j}$ species as a function of time from P_c and a first-order rate constant (k) defined by

$$k = k'(P^{18}O_4)/P_c \quad (4)$$

The oxygen exchange rate (v_{ex}) is the rate at which the second step in eq 1 reverses (Boyer et al., 1977):

$$v_{ex} = k_{-2}[E\text{–}P]_{ss} = k_{ex}[E]_0[P_i]_0/(K_m + [P_i]_0) \quad ([P_i]_0 \gg [E]_0) \quad (5)$$

$[E\text{–}P]_{ss}$ is the steady-state phosphoenzyme concentration, and the exchange parameters are

$$k_{ex} = k_2k_{-2}/(k_2 + k_{-2}) \quad (6)$$

and

$$K_m = k_{-1}k_{-2}/[k_1(k_2 + k_{-2})] \quad (7)$$

The measured exchange rate is less than v_{ex} unless $k_{-1} \gg k_2$, because re-forming E–P does not introduce water oxygens into medium P_i. v_{ex} was evaluated from the measured rate of disappearance (v_4) of the $P^{18}O_4$ isotopomer (Hackney, 1980):

$$v_4 = k'(P^{18}O_4)[P_i]_0 = (1 - P_c)v_{ex} \quad (8)$$

Best estimates of k_{ex} and K_m were obtained by a nonlinear

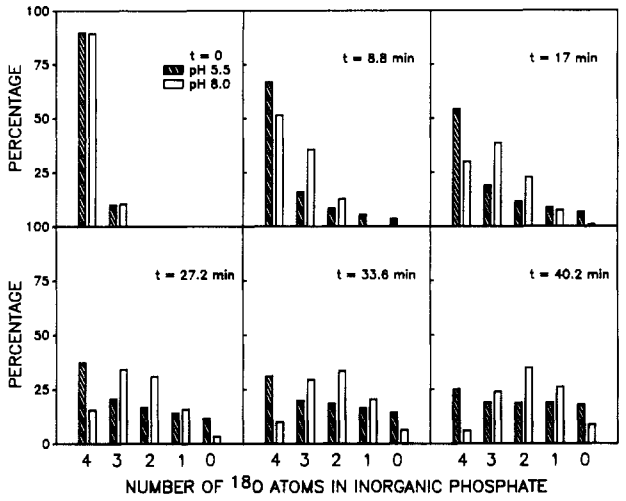

FIGURE 2: Effect of pH on $P^{18}O_j{}^{16}O_{4-j}$ distribution formed with time during catalysis of medium ^{18}O exchange by H,K-ATPase. The ^{31}P NMR spectrum of $[^{18}O]P_i$ was measured at pH 5.5 and 8.0. Other experimental conditions: 9.4 mM $[^{18}O]P_i$, 1 mM EDTA, 3 mM $MgCl_2$, 7 mM KCl, 50% D_2O, and 81 μg mL^{-1} protein in 40 mM MES buffer (pH 5.5) or 75 μg mL^{-1} protein in 40 mM imidazole buffer (pH 8.0), at 37 °C. In the figure, the percentage contribution of each isotopomer to the spectrum is represented in a bar graph. The individual bar graphs compare the distributions at pH 5.5 (diagonal filled bars) and pH 8.0 (unfilled bars) at the specified reaction times and comparable extents of reaction. The average isotope enrichment remaining after the longest time was 53.5% at pH 5.5 and 48.1% at pH 8.0.

least-squares fit of eq 8, with eq 5 substituted for v_{ex} and with P_c fixed at the mean value, to measurements of $k'(P^{18}O_4)$ as a function of $[P_i]_0$.

k_1 was calculated from the ratio of the estimated exchange parameters (eq 6 and 7):

$$k_1 = (k_{ex}/K_m)[(1 - P_c)/P_c] \quad (9)$$

If there really is only one intermediate in the formation of E–P, k_1 should approach the theoretical value for a diffusion-controlled bimolecular reaction.

Results

$P^{18}O_j{}^{16}O_{4-j}$ Distribution. There is a dramatic change in the distribution of $P^{18}O_j{}^{16}O_{4-j}$ isotopomers formed with time when H,K-ATPase catalyzes ^{18}O exchange out of $P^{18}O_4$ at different pH values. In Figure 2 bar graphs are used to compare the isotope distributions calculated from real time NMR measurements at pH 5.5 and 8.0. At the higher pH, isotopomers containing one less ^{18}O atom sequentially become the dominant species in the distribution (unfilled bars). In sharp contrast, at pH 5.5 unenriched P_i (zero ^{18}O atoms) forms before the fully labeled species (four ^{18}O atoms) has decayed significantly, and an isotopomer containing both ^{16}O and ^{18}O is never the dominant form of P_i (diagonal filled bars). At every pH semilogarithmic plots of percent $P^{18}O_4$ and percent AE versus time are linear for at least one half-time (Figure 3). Figure 4 compares the experimental data at an intermediate pH (6.6) with theoretical curves for catalysis of exchange by a single reaction pathway with the P_c and k calculated from Figure 3 by use of eq 3 and 4. The variation in P_c with pH is graphed in Figure 5. At pH 8 there is less than 1 chance in 10 that E–P will re-form before P_i dissociates, so the distribution of ^{18}O in P_i remains essentially random (Bock & Cohn, 1978). On the other hand, at pH 5.5 each phosphate molecule reacts covalently with the enzyme nearly twice, on the average, before it diffuses away, and the $P^{18}O_j{}^{16}O_{4-j}$ distribution becomes increasingly nonrandom with time. The pH dependence of

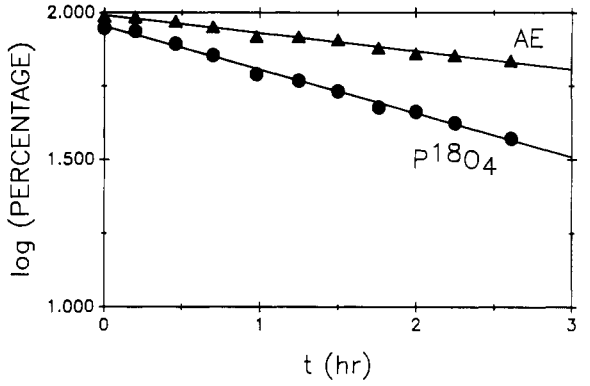

FIGURE 3: Catalyzed exchange of ^{18}O is first order. The logarithm of the percentage of P_i remaining as $P^{18}O_4$, or the percentage of the oxygen in P_i that is ^{18}O (AE), is plotted against time (t). The data are for pH 6.6, imidazole buffer, and 80 μg mL^{-1} protein. Other experimental conditions are given in the legend to Figure 2. The pseudo-first-order rate constants (k') evaluated from the slopes of the least-squares lines drawn through the experimental points were used to calculate the P_c (eq 3) and k (eq 4) values reported in the legend to Figure 4.

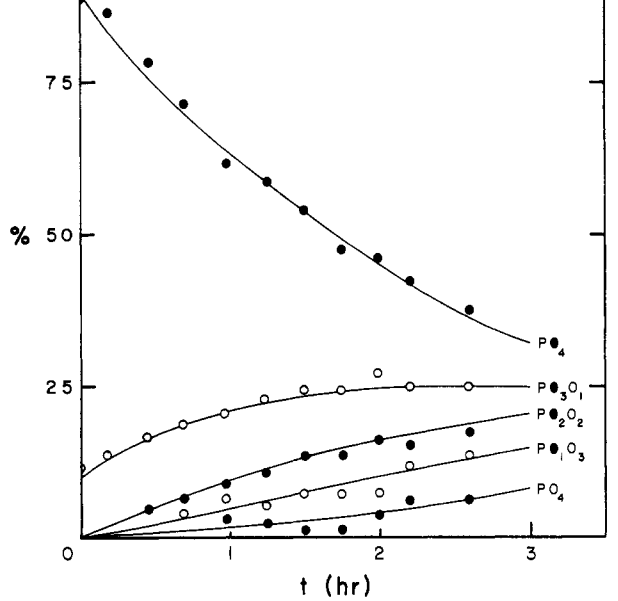

FIGURE 4: Fit of theory for medium ^{18}O exchange by a single reaction pathway to experimental $P^{18}O_j{}^{16}O_{4-j}$ distribution at pH 6.6. The percentage of P_i with the isotope distribution shown to the right of each curve (● denotes ^{18}O) is plotted against time. The theoretical curves were calculated with the equations derived by Hackney (1980) for $P_c = 0.5$, $k = 0.68$ h^{-1}, and the measured initial distribution 88.7% $P^{18}O_4$ and 11.3% $P^{18}O_3{}^{16}O_1$.

P_c is compared in the figure to the theoretical titration curve of a weak acid with $pK_a = 7.2$.

Exchange Rate. GCMS analysis of the $P^{18}O_j{}^{16}O_{4-j}$ distribution was used to measure the exchange rate as a function of $[^{18}O]P_i$ concentration. The results at pH 5.5 are shown in Figure 6. Within experimental error, the same P_c was measured at every P_i concentration. $P_c = 0.64 \pm 0.06$ ($n = 16$). The theoretical curve shows that the data satisfactorily conform to the hyperbolic dependence of v_4 on $[P_i]_0$ predicted by eq 5 and 8. The estimated values of k_{ex} and K_m are reported in Table I. Analogous measurements were made at three other pH values. The results are summarized in Table I. The mean values (± standard deviation) of P_c are plotted in Figure 5 (filled circles).

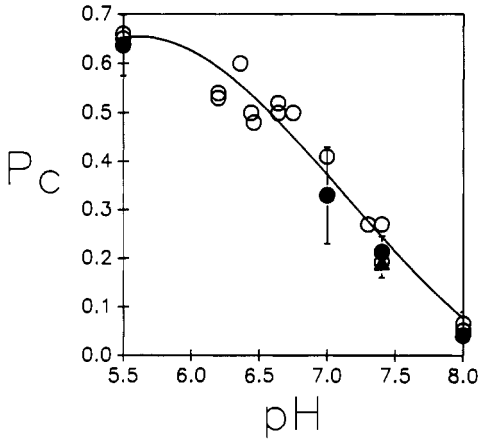

FIGURE 5: P_c for catalysis of medium ^{18}O exchange by H,K-ATPase as a function of pH. The P_c values denoted by unfilled circles (○) were calculated from real-time NMR measurements of the $P^{18}O_i^{16}O_4^{-}$ distribution. Experimental conditions: $30 \leq P_0 \leq 180$ μg mL^{-1}, 9.4 mM [^{18}O]P_i, 1 mM EDTA, 3 mM $MgCl_2$, 7 mM KCl, and 50% D_2O in 40 mM MES or imidazole buffer at 37 °C. The filled circles (●) indicate the mean and standard deviations (error bars) of P_c values determined at different P_i concentrations by GCMS. See Figure 6 legend for experimental details. The filled triangle (▲) is the mean ± standard deviation (error bar) of experiments in which K^+ was varied. P_c was calculated as described in the text. The solid line was calculated for titration of a weak acid with $pK_a = 7.2$.

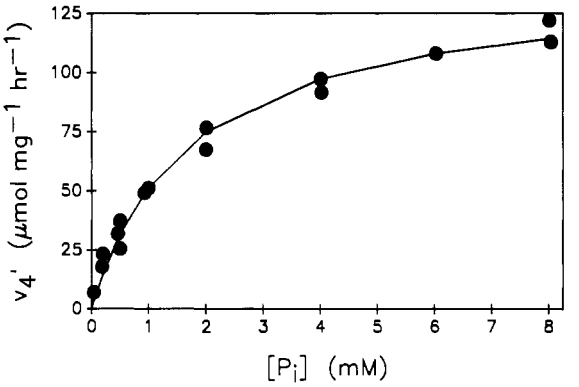

FIGURE 6: Variation of the exchange rate of the fully enriched isotopomer ($P^{18}O_4$) with P_i concentration. Specific rate ($v_4' = v_4/P_0$) is plotted. The theoretical line is the least-squares fit of eq 5 and 8 to the experimental data with $k = 382$ h^{-1} and $K_m = 1.7$ mM. Experimental conditions: $0.05 \leq [P_i] \leq 8$ mM, 10–56 μg of protein mL^{-1}, 2 mM $MgCl_2$, and 7 mM KCl in 40 mM MES buffer at pH 5.5 and 37 °C.

Table I: Summary of Exchange Parameters

pH	P_c	v_{ex}' [a] (μmol mg^{-1} h^{-1})	K_m (mM)	RMSE [b]
5.5	0.64	382	1.7	5.1
7.0	0.33	551	2.0	12.8
7.4	0.21	988	1.1	30.2
8.0	0.04	760	3.5	12.2
			⟨2.1 ± 1.0⟩	

[a] $v_{ex}' = v_4'(\max)/(1 - P_c) = k_{ex}$. [b] Root mean square error.

The exchange rate at a fixed $[P_i]_0$ was measured as a function of K^+ concentration. The results are shown in Figure 7. No attempt was made to calculate a theoretical curve, because the rate profile is bell-shaped. Therefore, the maximum velocity is uncertain. Inactivation occurs at such a high [K^+] that nonspecific binding, as well as specific binding, and ionic strength effects could be contributing. $P_c = 0.19 \pm 0.03$ ($n = 6$) did not vary with K^+ concentration. The mean value of P_c (± standard deviation) is plotted in Figure 5 (filled triangle).

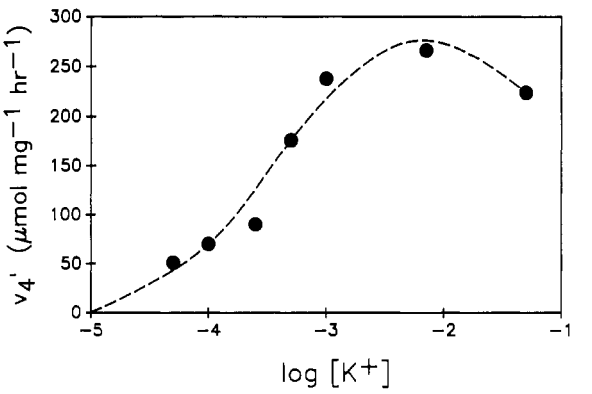

FIGURE 7: Dependence of ^{18}O exchange rate on K^+ concentration. The specific rate of $P^{18}O_4$ disappearance (v_4') is plotted against log [K^+]. Experimental conditions: 0.5 mM [^{18}O]P_i, $30 \leq P_0 \leq 150$ μg mL^{-1}, $0.05 \leq$ [KCl] ≤ 5 mM, and 2 mM $MgCl_2$ in 40 mM imidazole, pH 7.4, at 37 °C.

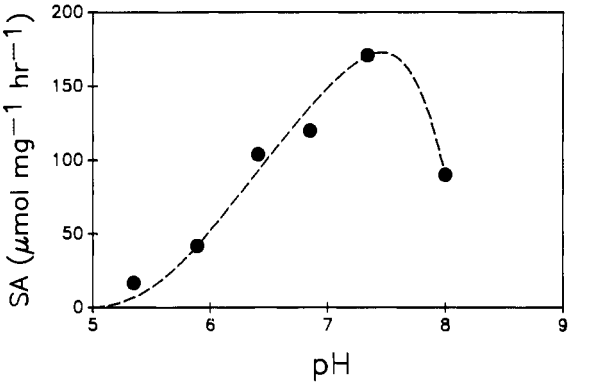

FIGURE 8: Effect of pH on ATPase activity of H,K-ATPase. Specific activity (SA) is plotted. Experimental conditions: 2 mM, ATP, 10–50 μg of protein mL^{-1}, 2 mM $MgCl_2$, and 7 mM KCl in 40 mM MES or imidazole buffer at 37 °C.

Specific Activity. A bell-shaped response was also obtained when the catalyzed rate of ATP hydrolysis was measured as a function of pH. This result is shown in Figure 8. The dashed curve can be simulated by assuming successive ionizations activate and inactivate the enzyme. A range of activation and inactivation constants are possible, depending upon the maximum rate chosen.

Discussion

The H,K-ATPase is classified as an E_1E_2-type ATPase. The distinguishing characteristic of these enzymes, which include the Na^+ and Ca^{2+} pumps, is that they catalyze active transport by forming a covalent phosphoenzyme intermediate. The designation E_1E_2 is derived from the currently favored explanation of catalysis–transport coupling and ion translocation. Two enzyme conformations are postulated that bind the transported ions tightly from different sides of the membrane and catalyze different partial reactions. This is shown diagrammatically in Figure 1 for transport of H^+ and K^+ ions. The scheme will not work if $E_1{\sim}P$ can react with HOH, because then ATP hydrolysis would be catalyzed without accompanying transport of ions (Jencks, 1980). Therefore, one consequence of the model is that medium ^{18}O exchange is catalyzed exclusively by the E_2 conformer of the enzyme. Predictable effects of the transported ions on the exchange reaction motivated the experiments reported in this study and provide a framework for discussing the results.

Effect of K^+ on Medium ^{18}O Exchange. The model predicts an increase in the medium exchange rate with K^+ concentration, because tighter binding of K^+ to E_2 shifts the equi-

Table II: Comparison of k_1 with Some Previously Reported Second-Order Rate Constants: a + b $\underset{k_r}{\overset{k_f}{\rightleftharpoons}}$ c

reaction	pH	k_1 (M^{-1} s^{-1})	k_f (M^{-1} s^{-1})	k_r (s^{-1})	ref
proflavin + proflavin			7.9×10^8	2.0×10^6	Turner et al., 1972
proflavin + chymotrypsin			4.1×10^7	1.7×10^3	Faller & Lafond, 1971
vanadate + Na,K-ATPase			6.5×10^4	3.3×10^{-3}	Cantley et al., 1978
vanadate + H,K-ATPase			2.0×10^4	2.5×10^{-3}	Faller et al., 1983
phosphate + H,K-ATPase	8.0	9.6×10^5			this study
	7.4	6.3×10^5			
	7.0	1.0×10^5			
	5.5	2.3×10^4			

librium between E_1 and E_2 increasing the fraction of the enzyme in the conformer that reacts with P_i. P_c should not change, because only the E_2 conformer catalyzes exchange. These predictions are confirmed. Half-maximum exchange occurs at approximately 0.3 mM K^+, but the actual activation constant could be higher because the reaction is inhibited above 7 mM K^+ (Figure 7). P_c is unaffected by K^+ concentration (Figure 5, filled triangle). Inhibition of exchange above 7 mM K^+ is not predicted by the model.

The E_1E_2 model's explanation of K^+ activation of exchange is supported by experimental evidence that K^+ binding with $K_d \geq 0.3$ mM causes conformational changes in the gastric H,K-ATPase. The reversibly bond fluorescent substrate analogue TNP-ATP reports a change in the enzyme's conformation induced by K^+ with $K_d = 3$ mM (Faller, 1989b). K^+ quenches the fluorescence of enzyme irreversibly inactivated by FITC with $K_d = 0.25$ mM (Jackson et al., 1983).

Effects of pH on Medium ^{18}O Exchange. A decrease in the estimated maximum exchange rate (Table I, $v_{ex}' = k_{ex}$) with pH is predicted by the E_1E_2 model, since tighter H^+ binding to E_1 decreases the fraction of the enzyme in the conformer that catalyzes medium ^{18}O exchange. This prediction is also confirmed. v_{ex}' at pH 5.5 is about 40% of the maximum value. In agreement with the sharper dependence of SA on pH shown in Figure 8, v_4 (Equation 8) decreases more dramatically than v_{ex}' because increasing [H^+] increases P_c (Table I). v_4' at pH 5.5 is about 15% of the maximum value. Inhibition of exchange above pH 7.4 is not predicted by the model.

Neither does the E_1E_2 model predict the inverse relationship between P_c and pH reported in Figure 5. The only way a change in P_c can be explained is by a different reaction mechanism, because P_c is a ratio of rate constants (eq 2). The observed increase in P_c with H^+ concentration (Figure 5) indicates that k_2 increases relative to k_{-1}. Whether the dominant effect of protons is to increase the rate of phosphoenzyme formation or decrease the rate of P_i dissociation cannot be decided by measurements of the $P^{18}O_j{}^{16}O_{4-j}$ distribution. Neither possibility could be explained by protons shifting the equilibrium between E_1 and E_2, because only one conformer (E_2) catalyzes ^{18}O exchange according to the model. If the model were wrong and E_1 catalyzed isotope exchange by a different mechanism, the result in Figure 4 would be unexpected.

The observed dependence of the isotopomer distribution on time at intermediate pH values can be described by a single P_c (Figure 4). Therefore, the continuous variation of P_c with pH shown in Figure 5 must result from a reaction that is fast compared to the P_i off-rate. There are three limiting possibilities: (1) protonation of the substrate, (2) protonation of a group on the enzyme, or (3) rapid interconversion of $E_1{\cdot}P_i$ and $E_2{\cdot}P_i$. Only the third possibility is incompatible with the E_1E_2 model, because E_1 would also have to catalyze exchange for P_c to vary. It is the least likely explanation, since a conformational change both extensive enough to bind ions and then release them on different sides of a membrane and faster than the P_i off-rate is hard to envision.

The theoretical titration curve in Figure 5 shows that ionization of a weak acid with $pK_a = 7.2$ could explain the experimentally observed change in P_c with pH. Since the second acid dissociation constant of P_i is 6.71 (Schwarzenbach & Geier, 1963), one possibility is that $H_2PO_4^{2-}$ and HPO_4^- react by different mechanisms. This explanation is complicated by the coordination reaction of Mg^{2+} with P_i. The true substrate of the Ca-ATPase is the metal coordination complex (Champeil et al., 1985). The absolute formation constant of $MgHPO_4$ is 1.88 (Smith & Alberty, 1953), so the relative amounts of MgP_i and P_i may have varied significantly in the measurements of exchange rate as a function of P_i concentration at the higher pH values investigated in this study. Nevertheless, eq 5 and 8 fit the rate data satisfactorily at every pH (Table I).

Hyperbolic variation of the measured exchange rate with total P_i concentration suggests that protonation of a weakly acidic group on the enzyme may be more important in explaining the increase in P_c with H^+ (Figure 5) than protonation or metal coordination of P_i in the case of the H,K-ATPase. The obvious candidate is the imidazole side chain of histidine, but other functional groups may titrate near neutrality in a protein environment. Support for attributing the observed variation of P_c with pH to ionization of a group on the enzyme is provided by studies of the effect of pH on phosphorylation of the H,K-ATPase by [γ-^{32}P]ATP and subsequent breakdown of the phosphoenzyme intermediate (Stewart et al., 1981; Ljungstrom et al., 1984). The results were explained by ionization of a weakly acidic group on the enzyme, because K^+ competed with H^+ and H^+ affected phosphorylation and dephosphorylation from different sides of the membrane.

Evidence for a Slow Step in the Catalytic Mechanism. The number of reactive sites is needed to calculate k_1 in units of M^{-1} s^{-1} from eq 9 with the estimates of k_{ex}, K_m, and P_c reported in Table I. Since the level of ^{32}P incorporation into the gastric H,K-ATPase from [^{32}P]P_i has not been measured, the stoichiometry of E–P formation from ATP was used to calculate the k_1 values recorded in Table II. A variety of inhibitors of the H,K-ATPase, including several substrate analogues, bind with twice the phosphorylation stoichiometry (Faller, 1989a), so the numbers quoted may be off by a factor of 2. Uncertainty about the active site stoichiometry cannot account for the observed trend in k_1 with pH.

In Table II the estimates of k_1 are compared to some measured forward rate constants (k_f). The reactions of proflavin are nearly diffusion controlled. That is, k_f approaches the theoretical maximum value ($k_{f,D}$) for bimolecular association of molecules that size and charge in solution (Eigen & Hammes, 1963). The measured k_f will be less than $k_{f,D}$ if diffusional encounter is followed by a slower chemical transformation. For example, it is clear an intermediate and a slow step are involved in formation of the noncovalent

Table III: Comparison of Estimated Rate Constants for H,K-ATPase with Published Values for Phosphorylation of the Ca-ATPase by P_i

enzyme	k_1 (M^{-1} s^{-1})	k_{-1} (s^{-1})	k_2 (s^{-1})	k_{-2} (s^{-1})	ref
H,K-ATPase	6.3×10^5	1.1×10^3	305	457	this study[a]
Ca-ATPase	2.8×10^5	378	32	51	McIntosh & Boyer, 1983[b]
	1.5×10^4	140	21	23	Pickart & Jencks, 1984[c]
	2.0×10^5	300	250	0.8	Champell et al., 1985[d]

[a] pH 7.4; $[E-P]_{ss}$ = 0.6 nmol mg^{-1}. [b] pH 6.5; 70% of the protein is enzyme; MW = 100 kDa. [c] pH 6.0. [d] pH 6.0; 15% DMSO.

complex between vanadate and the H,K-ATPase, because the half-time for the reverse reaction is 4.6 min.

The k_1 calculated with eq 9 is k_f for formation of the E·P_i intermediate that loses HOH. The possibility that k_f approaches $k_{f,D}$ at pH 8 cannot be excluded, because some of the information needed to calculate $k_{f,D}$ for a reaction with an integral membrane protein, like the diffusion coefficient of membrane vesicle fragments, is unavailable. However, it is unlikely changes in charge or mobility with pH can account for the calculated decrease in k_1. At pH 5.5, k_1 approximately equals k_f for vanadate reaction with the enzyme. The decrease in k_1 with pH to a value smaller than expected for a collisional encounter is compatible with an additional step involving a slow chemical transformation and another intermediate in the catalytic mechanism.

One possibility for this additional step is a protein conformational change. There is experimental evidence P_i binding causes conformational changes in both the sodium and calcium pumps. For example, large enthalpy and entropy changes when P_i binds to the Na,K-ATPase (Kuriki et al., 1976), or Ca-ATPase (Epstein et al., 1980), were explained by a conformational change. The authors proposed that the P_i binding energy is required to drive phosphorylation of an aspartyl group in these enzymes by P_i, because reaction of P_i with carboxylic acids is endergonic. The k_1 values found for the H,K-ATPase at the lower pH values fall in the range reported for the Ca-ATPase (Tables II and III).

Comparison with Other E_1E_2 ATPases. The remaining rate constants in the simplest phosphorylation mechanism (eq 1) can also be estimated from the ^{18}O exchange data. k_{-2} can be obtained from the exchange rate by eq 5, if $[E-P]_{ss}$ is known. Then k_2 can be calculated from eq 6 and k_{-1} from eq 2. The steady-state level of E–P formed from P_i has not been measured, and there is only limited information about the steady-state concentration of E–P during ATP hydrolysis when K^+ is present. Nevertheless, it is worthwhile to estimate the rate constants for phosphorylation of the H,K-ATPase by the scheme in eq 1 and compare them to values reported for phosphorylation of the Ca-ATPase by the same mechanism. The numbers quoted for the H,K-ATPase were calculated by assuming 40% of the available sites are phosphorylated in 7 mM KCl (Wallmark & Mardh, 1978).

The estimates of the rate constants for phosphorylation of the H,K-ATPase by P_i are compared with published values for the Ca-ATPase in Table III. The agreement is quite good. Differences in the numerical values reported for the two enzymes can be attributed partly to different assumptions about the number of reactive sites. For example, basing calculations for the H,K-ATPase on molecular weight, and assuming 70% of measured protein is enzyme, gives $k_1 = 1.5 \times 10^5$ M^{-1} s^{-1}, $k_{-1} = 1.1 \times 10^3$ s^{-1}, $k_2 = 76$ s^{-1}, and $k_{-2} = 111$ s^{-1}. pH also affects the numerical values of the rate constants. The v_{ex} versus pH profile of the Ca-ATPase is bell shaped. Taking an increase in v_{ex} with pH and a change in phosphoenzyme level (de Meis, 1976) into account, k_{-2} varies from 17 s^{-1} at pH 6 to 112 s^{-1} at pH 7. P_c increased from 0.02 at pH 7 to 0.33 at pH 5.4 (McIntosh & Boyer, 1983). The $P^{18}O_j{}^{16}O_{4-j}$ distribution remains nearly random ($0.01 \leq P_c \leq 0.03$) when the Na,K-ATPase catalyzes medium exchange at pH 7.2. At pH 6.6 v_{ex} is reduced 70%, and two to three oxygen atoms exchange per bound P_i (Dahms & Miara, 1983). This corresponds to a P_c between 0.8 and 0.9 and represents an even more dramatic change in mechanism with pH than found for the H,K-ATPase.

Summary. The conformational model of coupled, vectorial transport (Figure 1) predicts the effects of K^+ on catalysis of medium ^{18}O exchange by the H,K-ATPase, except for the decrease in v_{ex} above 7 mM K^+. It predicts the observed decrease in v_{ex} below pH 7.4 but not the decrease in v_{ex} above pH 7.4 or the measured change in P_c with pH. Evidence for two new features of the catalytic mechanism of the H,K-ATPase is presented in this study. First, slower than diffusion-controlled formation of the E·P_i complex that exchanges ^{18}O with HOH is consistent with a slow step involving an additional intermediate in the phosphorylation mechanism.

$$E + P_i \rightleftharpoons E{\cdot}P_i \rightleftharpoons E'{\cdot}P_i \rightleftharpoons E'{-}P + HOH$$

There is precedent from microcalorimetric studies (Kuriki et al., 1976; Epstein et al., 1980) for a conformational change with P_i binds to other E_1E_2-type enzymes that may be important in explaining the energetics of phosphorylation by inorganic phosphate. Second, a single P_c that depends on pH like a single-group titration (Figure 5) is evidence for participation of a weak acid in the reaction mechanism. This study is the first demonstration that the mechanism actually changes when a group is protonated, because faster phosphorylation by ATP at low pH (Stewart et al., 1981; Ljungstrom et al., 1984) could be explained by an increase in the fraction of the enzyme in the E_1 conformer that reacts with ATP.

Acknowledgments

We are indebted to Jane Strouse for help with the NMR measurements, to Kerstin Stempel for instruction in the preparation of $[^{18}O]P_i$ and GCMS measurements, and to Professor Paul Boyer for his encouragement and many helpful discussions.

References

Bock, J. L., & Cohn, M. (1978) *J. Biol. Chem. 253*, 4082–4085.

Boyer, P. D., de Meis, L., Carvalho, M., & Hackney, D. D. (1977) *Biochemistry 16*, 136–140.

Cantley, L. C., Jr., Cantley, L. G., & Josephson, L. (1978) *J. Biol. Chem. 253*, 7361–7368.

Champeil, Ph., Guillain, F., Venien, C., & Gingold, M. P. (1985) *Biochemistry 24*, 69–81.

Cohn, M., & Hu, A. (1978) *Proc. Natl. Acad. Sci. U.S.A. 75*, 200–203.

Dahms, A. S., & Miara, J. E. (1983) *Curr. Top. Membr. Transp. 19*, 371–375.

de Meis, L. (1976) *J. Biol. Chem. 251*, 2055–2062.

Eigen, M., & Hammes, G. G. (1963) *Adv. Enzymol. Relat. Areas Mol. Biol. 25*, 14–51.

Epstein, M., Kuriki, Y., Biltonen, R., & Racker, E. (1980) *Biochemistry 19*, 5564–5568.

Faller, L. D. (1987) *Biophys. J. 51*, 3885a.
Faller, L. D. (1989a) *Biochemistry 28*, 6771-6778.
Faller, L. D. (1989b) *Biochemistry* (submitted for publication).
Faller, L. D., & LaFond, R. E. (1971) *Biochemistry 10*, 1033-1041.
Faller, L. D., Rabon, E., & Sachs, G. (1983) *Biochemistry 22*, 4676-4685.
Faller, L. D., & Elgavish, G. A. (1984) *Biochemistry 23*, 6584-6590.
Hackney, D. D. (1980) *J. Biol. Chem. 255*, 5320-5328.
Hackney, D. D., & Boyer, P. D. (1978) *Proc. Natl. Acad. Sci. U.S.A. 75*, 3133-3137.
Hackney, D. D., Stempel, K. E., & Boyer, P. D. (1980) *Methods Enzymol. 64*, 60-83.
Jackson, R. J., Mendlein, J., & Sachs, G. (1983) *Biochim. Biophys. Acta 731*, 9-15.
Jencks, W. P. (1980) *Adv. Enzymol. Relat. Areas Mol. Biol. 51*, 75-106.
Kuriki, Y., Halsey, J., Biltonen, R., & Racker, E. (1976) *Biochemistry 15*, 4956-4961.
Ljungstrom, M., Vega, F. V., & March, S. (1984) *Biochim. Biophys. Acta 769*, 220-230.
Lowry, O. H., Rosenbrough, N. J., Farr, A. L., & Randall, R. J. (1951) *J. Biol. Chem. 193*, 265-275.
McIntosh, D. B., & Boyer, P. D. (1983) *Biochemistry 22*, 2867-2875.
Pickart, C. M., & Jencks, W. P. (1984) *J. Biol. Chem. 259*, 1629-1643.
Schwarzenbach, G., & Geier, G. (1963) *Helv. Chim. Acta 46*, 906-926.
Shull, G. E., & Lingrel, J. B. (1986) *J. Biol. Chem. 261*, 16788-16791.
Smith, R. M., & Alberty, R. A. (1956) *J. Am. Chem. Soc. 78*, 2376-2380.
Stempel, K. E., & Boyer, P. D. (1986) *Methods Enzymol. 126*, 618-639.
Stewart, B., Wallmark, B., & Sachs, G. (1981) *J. Biol. Chem. 256*, 2682-2690.
Turner, D. H., Flynn, G. W., Lundberg, S. K., Faller, L. D., & Sutin, N. (1972) *Nature 239*, 215-217.
Wallmark, B., & Mardh, S. (1979) *J. Biol. Chem. 254*, 11899-11902.
Yoda, A., & Hokin, L. E. (1980) *Biochem. Biophys. Res. Commun. 40*, 880-884.

Escherichia coli cAMP Receptor Protein: Evidence for Three Protein Conformational States with Different Promoter Binding Affinities†

Tomasz Heyduk and James C. Lee*
E. A. Doisy Department of Biochemistry, St. Louis University School of Medicine, 1402 South Grand Boulevard, St. Louis, Missouri 63104

Received February 27, 1989; Revised Manuscript Received May 5, 1989

ABSTRACT: Cyclic AMP receptor protein (CRP) from *Escherichia coli* is assumed to exist in two states, namely, those represented by the free protein and that of the ligand–protein complex. To establish a *quantitative* structure–function relation between cAMP binding and the cAMP-induced conformational changes in the receptor, protein conformational change was quantitated as a function of cAMP concentration up to 10 mM. The protein conformation was monitored by four different methods at pH 7.8 and 23 °C, namely, rate of proteolytic digestion by subtilisin, rate of chemical modification of Cys-178, tryptophan fluorescence, and fluorescence of the extrinsic fluorescence probe 8-anilino-1-naphthalenesulfonic acid (ANS). Each of these techniques reveals a biphasic dependence of protein conformation on cAMP concentration. At low cAMP concentrations ranging from 0 to 200 μM, the rates of proteolytic digestion and that of Cys-178 modification increase, whereas the fluorescence intensity of the ANS–protein complex is quenched, and there is no change in the fluorescence intensity of the tryptophan residues in the protein. At higher cAMP concentrations, the rates of proteolytic and chemical modification of the protein *decrease*, while the fluorescence intensity of the ANS–protein complex is further quenched but there is an *increase* in the intensity of tryptophan fluorescence. These results show unequivocally that there are at least three conformational states of the protein. The association constants for the formation of CRP–cAMP and CRP–$(cAMP)_2$ complexes derived from conformational studies are in good agreement with those determined by equilibrium dialysis, nonequilibrium dialysis, and ultrafiltration. Therefore, the simplest explanation would be that the protein exhibits three conformational states, free CRP and two cAMP-dependent states, which correspond to the CRP–cAMP and CRP–$(cAMP)_2$ complexes. The binding properties of CRP–cAMP and CRP–$(cAMP)_2$ to the *lac* promoter were studied by using the gel retardation technique. At a high concentration of cAMP which favors the formation of the CRP–$(cAMP)_2$ complex, binding of the protein to DNA is decreased. This, together with conformational data, strongly suggests that only the CRP–cAMP complex is active in specific DNA binding whereas CRP and CRP–$(cAMP)_2$ are not.

Cyclic AMP receptor protein (CRP)[1] from *Escherichia coli* plays a key role in the regulation of expression of more than 20 genes in bacteria. The basic mechanism involves binding of CRP to the promoter regions of these genes. The formation of these CRP–DNA complexes is allosterically regulated by cAMP. There is ample evidence to indicate that binding of

† Supported by NIH Grants NS-14269 and DK-21489.

[1] Abbreviations: CRP, cyclic AMP receptor protein; ANS, 8-anilino-1-naphthalenesulfonic acid; DTNB, 5,5′-dithiobis(2-nitrobenzoic acid); TNB, 2-nitro-5-thiobenzoate; PMSF, phenylmethanesulfonyl fluoride; SDS, sodium dodecyl sulfate.

0006-2960/89/0428-6914$01.50/0